PCCP

Accepted Manuscript

ROYAL SOCIETY OF CHEMISTRY

www.rsc.org/pccp

Journal Name

ARTICLE TYPE

Cite this: DOI: 10.1039/xxxxxxxxxx

Exploring the Role of the 3-Center-4-Electron Bond in Hypervalent λ^3-Iodanes Using the Methodology of Domain Averaged Fermi Holes†

Halua Pinto de Magalhães,[a] Hans Peter Lüthi,*[a] and Patrick Bultinck[b]

Received Date
Accepted Date

DOI: 10.1039/xxxxxxxxxx

www.rsc.org/journalname

Hypervalent iodine compounds, in particular λ^3-iodanes, have become important reagents in organic synthesis for the electrophilic transfer of substituents to arenes and other nucleophiles. The structure and reactivity of these compounds are usually described based on a 3-center-4-electron bond model , involving the iodine central atom and its two *trans* substituents.

The goal of this computational study is to explore Fermi correlation in view of a more advanced description of bonding in these compounds. For that matter, we apply the analysis of Domain Averaged Fermi Holes (DAFH). The DAFH analysis revealsa relationship between the occurrence of multicenter bonding and structural parameters which cannot easily be observed based on simple MO theory. Whereas for λ^3-iodanes carrying electron-rich ligands pairing of electrons over three centers is indeed observed, compounds with electron-withdrawing substituents fall into a different category: the pairing of electrons is restricted to extend over two centers only, thus challenging the multicenter bonding picture in this case. Accordingly, a drastic reduction of the DAFH 3-center index is observed.

The establishment of the multicenter bond in λ^3-iodanes is driven by a pseudo Jahn-Teller (PJT) effect, whose extent is tightly coupled to the reactivity of the corresponding compound. The PJT stabilization scales with the degree of s-p hybridization of the central atom, which, in return, depends on the electron-withdrawing power of the ligands in *trans* position. The response of the multicenter bond to the iodine "ligand field" can be expressed quantitatively in terms of DAFH bond indices. These show, for example, that the activation of the reacting hypervalent species by means of protonation results in a weaker 3-center 4-electron bond, thus making the reagent more reactive.

In this work we explain a number of experimentally known facts concerning the reactivity of these compounds. We also show that the DAFH analysis offers a more complete understanding of hypervalency in λ^3-iodanes, and that it is a tool to assist the search for novel reagents.

1 Introduction

Hypervalent iodine compounds, in particular λ^3-iodanes, have become important reagents in organic synthesis for the electrophilic transfer of substituents to a variety of nucleophiles.[1] One example is the "Togni reagent" 3,3-Dimethyl-1-(trifluoromethyl)-1λ^3,2-benziodoxol (DMTB) *(1a)* used for the trifluoromethylation of a wide array of target compounds including proteins.[2] Another example are diaryliodanes, which easily isomerize and are used for selective functionalization of arenes *(1b)*. These and other reagents, including model compounds in their equilibrium and transition state (TS) geometry *(1c and d)*, are the topic of the present work.

It is not until recently that these hypervalent compounds, whose reactivity is reminiscent of organometallics, were the subject of elaborate mechanistic studies.[3–6] The reactivity of these reagents is governed by the electronic structure of the hypervalent region with the iodine atom as central atom. The interaction between the iodine atom and its *trans* substituents in a λ^3-iodane is usually described in terms of a 3-center-4-electron (3c-4e) bond model as presented by Hach, Rundle and Pimentel.[7,8] According to this model, the three molecular orbitals (MOs) governing this

[a] Department of Chemistry and Applied Biosciences, ETH Zürich, Vladimir-Prelog-Weg 2, CH-8093 Zürich, Switzerland. E-mail: hans.luethi@phys.chem.ethz.ch
[b] Department of Inorganic and Physical Chemistry, Ghent University, Krijgslaan 281, B-9000 Gent, Belgium

† Electronic Supplementary Information (ESI) available: [details of any supplementary information available should be included here]. See DOI: 10.1039/b000000x/

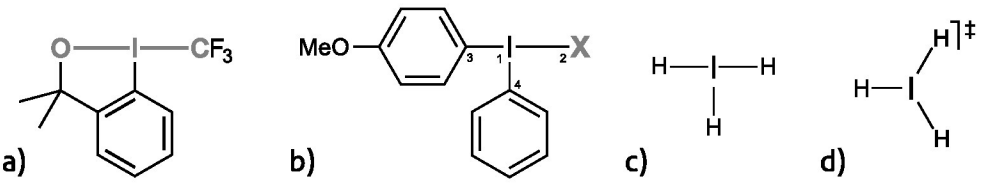

Fig. 1 a) 3,3-Dimethyl-1-(trifluoromethyl)-1λ^3,2-benziodoxol (DMTB), a reagent for the electrophilic transfer of the trifluoromethyl group by reductive elimination. b) 4-Methoxyaryl-phenyl-λ^3-iodane (diaryliodane) are used for the functionalization of arenes by *X*. c) The model compound IH_3 in its T-shape equilibrium geometry and, d) the corresponding Y-shape isomerization TS. a-c) These iodanes contain a 3-center-4-electron bond, involving the iodine atom and the two bonded atoms in *trans* configuration.

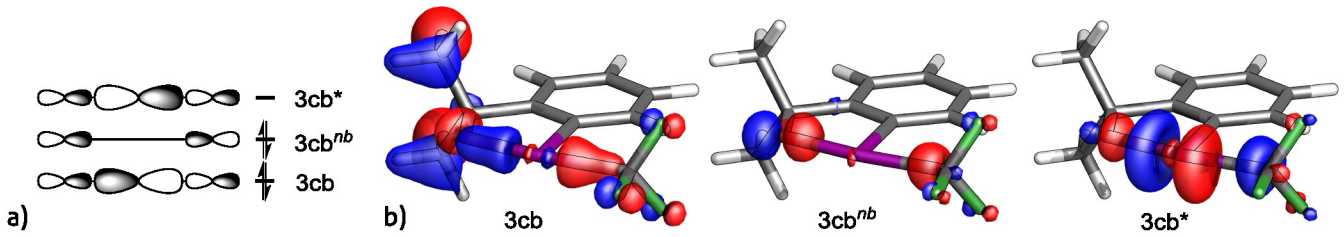

Fig. 2 a) The 3-center-4-electron bond model, and b) the 3-center canonical molecular orbitals (CMOs) of DMTB.

interaction exhibit bonding, non-bonding, and anti-bonding character in this order on the energy scale *(see 2a)*. The two lower-energy MOs are occupied by two electrons each, and the node at the iodine center of the non-bonding MO is responsible for the strongly polarized hypervalent bonds *(2)*. The third substituent is bound to the iodine through a classical 2-center bond.[9,10]

This MO based model allowed to understand many structural and electronic features of these compounds. In particular, we were able to show why the T-shape λ^3-iodanes isomerize via a Y-shape geometry, and why in chemical reactions retention of planarity of the hypervalent region is beneficial in view of low reaction barriers.[3] If planar TS are not accessible, the reductive elimination of the substituent *(CF_3 or X in 1, a and b)* is challenged by other reaction channels such as arene-coupling or radical mechanisms *(see Figure 3 in reference [3])*.

The height of the isomerization barrier as well as the planarity of the transition states are related to a pseudo Jahn-Teller (PJT) effect:[3] Distortion of a highly symmetric structure leads to symmetry induced orbital mixing between occupied and virtual orbitals resulting in the stabilization of the lower symmetry configuration.[11,12] As recently shown for the model compound IH_3, the in-plane distortion of the high symmetry Y-shape (D_{3h}) geometry towards a T-shape (C_{2v}) structure *(see 1c & d)* leads to the stabilization of the $3cb^{nb}$ orbital *(2a)* through interaction with a virtual orbital of the same symmetry (a_1).[3] The out-of-plane distortion of the D_{3h} structure towards a pyramidal (C_{3v}) configuration, on the other hand, comes with an energy penalty due to unfavorable mixing of the non-bonding $3cb^{nb}$ orbital with an occupied lone pair orbital of the iodine center *(for more detail see Figures 9 & 10 in reference [3])*.

Hypervalent bonding as found in λ^3-iodanes is observed in molecules containing main group elements (groups 13-18) that violate the Lewis octet rule by having more than eight electrons in their valence shell.[13,14] This phenomenon is due to the atomic shell structure, that is, the relative disparity of the radial extent of the valence *s*- and *p*-shells.[15,16] Later *p*-block elements exhibit so-called "hybridization defects" and also incorporate as little *s*-character in their bonding orbitals as possible. Thus, in these elements pure *p*-bonding is generally favored and the resulting hypervalent bonds are stabilized by multicenter bonding with a shared *p*-orbital of the central atom.[16]

However, multicenter bonding in hypervalent compounds is still the subject of an ongoing debate, and the different approaches often lead to contradictory views.[10,15–17] In the context of this work, we should mention an earlier investigation of SF_4 and PF_5 by Ponec et al., who, using an early implementation of the methodology of Domain Averaged Fermi Holes (DAFH), challenges the relevance of multicenter character in hypervalent bonding in those systems.[18,19] Dunning and co-workers present similar arguments against multicenter bonding within their approach for studying hypervalency in the framework of General Valence Bond (GVB) theory.[20] The "recoupled pair bond dyad" corresponds to two very polar but equivalently localized 2-center bonds, which is in contrast to the delocalized 3c-4e bond. Recently, Kaupp argued that the partially ionic resonance structures in VB language are equivalent to multicenter bonding in MO language, illustrating that the debate is not yet closed.[16]

The systems presented in this study are an extended series of iodanes, containing model systems such as IH_3 and IF_3, as well as diaryliodane systems, whose chemistry was previously explored in detail.[2–4,21,22] In these compounds, a 3c-4e bonding pattern, as described by the canonical molecular orbitals, allowed to explain the most important structure-bonding relationships. However, for the prediction of compound-specific features of the reactivity, the 3c-4e bond model is too general to serve as a good descriptor. Hence, the goal of the present study is to explore the DAFH analysis as a tool to gain more insight in the electronic structure of λ^3-iodanes, and to reach a better understanding of the reactivity of there compounds.

2 Theoretical Framework of Domain Averaged Fermi Holes

The electronic wave function, obtained as an (approximate) eigenfunction of the Hamiltonian operator, contains all information on the electronic structure of a molecule, including the correlated behaviour of electrons. As is well-known, by going from classical to quantum mechanics and given a proper (approximate) wave function, the joint probability of finding two electrons at coordinates $\mathbf{x}_1$ and $\mathbf{x}_2$ differs from the product of the individual probabilities for each electron separately. It is in this departure from classical behaviour that the chemical bond finds its roots. The exchange-correlation hole matrix $h^{xc}(\mathbf{x}_1,\mathbf{x}_2;\mathbf{x}'_1,\mathbf{x}'_2)$ is a two-electron measure that reflects this non-classical behaviour, defined here as:

$$h^{xc}(\mathbf{x}_1,\mathbf{x}_2;\mathbf{x}'_1,\mathbf{x}'_2)=\rho(\mathbf{x}_1,\mathbf{x}'_1)\rho(\mathbf{x}_2,\mathbf{x}'_2)-2\rho^{(2)}(\mathbf{x}_1,\mathbf{x}_2;\mathbf{x}'_1,\mathbf{x}'_2) \quad (1)$$

In equation (1), $\rho(\mathbf{x}_i,\mathbf{x}'_i)$ is the first order density matrix where $\mathbf{x}_i$ stands for the collection of both spatial and spin coordinates of electron i ($\mathbf{x}_i=\mathbf{r}_i\sigma_i$) and $\rho^{(2)}(\mathbf{x}_1,\mathbf{x}_2;\mathbf{x}'_1,\mathbf{x}'_2)$ is the second order density matrix. Note that $h^{xc}(\mathbf{x}_1,\mathbf{x}_2;\mathbf{x}'_1,\mathbf{x}'_2)$ is an extension[23] of the more often encountered exchange-correlation hole to a matrix formulation to allow obtaining properly defined eigenvalues and eigenvectors. Also note that often slightly different expressions may be found depending on the normalisation considered in the definition of the second order density matrix $\rho^{(2)}(\mathbf{x}_1,\mathbf{x}_2;\mathbf{x}'_1,\mathbf{x}'_2)$ (here $\frac{N(N-1)}{2}$ with N the number of electrons) and depending on the sign chosen in $h^{xc}(\mathbf{x}_1,\mathbf{x}_2;\mathbf{x}'_1,\mathbf{x}'_2)$. $h^{xc}(\mathbf{x}_1,\mathbf{x}_2;\mathbf{x}'_1,\mathbf{x}'_2)$ clearly integrates to N and captures the essence of chemical bonding even already at the level of single determinant theory. Notably, an electron with given spin σ_i "digs a hole" around itself where the probability of finding another electron with the same spin is strongly reduced[24]. Based on this observation, Ponec et al.[25,26] derived the so-called Domain Averaged Fermi Hole analysis where first one limits $h^{xc}(\mathbf{x}_1,\mathbf{x}_2;\mathbf{x}'_1,\mathbf{x}'_2)$ to the case where all electronic coordinates have the same spin. This results in a spinless $g^{xc}(\mathbf{r}_1,\mathbf{r}_2;\mathbf{r}'_1,\mathbf{r}'_2)$:

$$g^{xc}(\mathbf{r}_1,\mathbf{r}_2;\mathbf{r}'_1,\mathbf{r}'_2)=\sum_{\sigma_1,\sigma_2}\int \mathrm{d}\omega_1\,\mathrm{d}\omega_2\;\delta_{\sigma_1\sigma_2}\,h^{(xc)}(\mathbf{r}_1\sigma_1,\mathbf{r}_2\sigma_2;\mathbf{r}'_1\sigma_1,\mathbf{r}'_2\sigma_2) \quad (2)$$

This way, one can examine, given a specific spin and position of one of the electrons (say $\mathbf{r}_1=\mathbf{r}'_1$), the exchange correlation hole as a function of the position of the other electron with the same spin (say $\mathbf{r}_2=\mathbf{r}'_2$). $g^{xc}(\mathbf{r}_1,\mathbf{r}_2;\mathbf{r}'_1,\mathbf{r}'_2)$ may be split in an α and a β part depending on the spin involved but for simplicity and given that all systems treated here are closed shells, we do not makes this distinction. The second, key idea in DAFH is to condense the functions derived from the holes $g^{xc}(\mathbf{r}_1,\mathbf{r}_2;\mathbf{r}'_1,\mathbf{r}'_2)$ to some spatial domain Γ in the molecule. The resulting $g^{xc}_\Omega(\mathbf{r}_2;\mathbf{r}'_2)$ are obtained through integration of $g^{xc}(\mathbf{r}_1,\mathbf{r}_2;\mathbf{r}'_1,\mathbf{r}'_2)$ over, say, electron 1 in a specific domain Γ in the molecule, often a single atom in the molecule (AIM):

$$g^{xc}_\Omega(\mathbf{r}_2;\mathbf{r}'_2)=\int g^{xc}(\mathbf{r}_1,\mathbf{r}_2;\mathbf{r}'_1,\mathbf{r}'_2)w_\Omega(\mathbf{r}_1)\,\delta\left(\mathbf{r}_1-\mathbf{r}'_1\right)\mathrm{d}\mathbf{r}_1\,\mathrm{d}\mathbf{r}'_1 \quad (3)$$

In Eq. (3) the integration is assumed to be expressible in terms of a 3D-domain in position space using a domain weight function w_Ω although equivalent expressions can be derived in Hilbert space to yield a Mulliken[27] type DAFH.[25,26] Moreover, also in 3D position space defined AIM, different results may be found[23] depending on whether one uses e.g., QTAIM[28–30] or Hirshfeld-I[31–34]. The latter differences are, however, fairly limited and in the remainder we use QTAIM throughout. Eq. (3) becomes particularly simple at the single Slater determinant level of theory, as in Hartree-Fock theory, thanks to the Löwdin relationship between density matrices of increasing order.[35,36] The same equations result from a Kohn-Sham Density Functional Theory approach although one should take in to account that there the Slater determinant can not be considered to stand on the same footing as in Hartree-Fock theory. Nevertheless, experience[37] has shown that very useful insight may be obtained from Kohn-Sham based delocalization indices which are based on DAFH. At the single determinant level, the following expression is found:

$$g^{xc}_\Omega(\mathbf{r}_2;\mathbf{r}'_2)=\sum_{ij}^{occ,\alpha}\phi_i(\mathbf{r}_2)S^{\Omega,\alpha}_{ij}\phi^*_j(\mathbf{r}'_2)+\sum_{ij}^{occ,\beta}\phi_i(\mathbf{r}_2)S^{\Omega,\beta}_{ij}\phi^*_j(\mathbf{r}'_2) \quad (4)$$

Here ϕ are the spatial parts of the spin orbitals and the integration was performed over a domain Ω that may be a single atom or a union of atoms. We also split the sum in two parts for spin α and spin β and sum only over the occupied orbitals with that spin. $S^{\Omega,\sigma}_{ij}$ is an element of the so-called Domain Overlap Matrix (better known as Atomic Overlap Matrix if the domain contains only a single atom):

$$S^{\Omega,\sigma}_{ij}=\int\phi^*_i(\mathbf{r}_1)w_\Omega(\mathbf{r}_1)\phi_j(\mathbf{r}_1)\,\mathrm{d}\mathbf{r}_1 \quad (5)$$

where AOM for spin α and β can be distinguished depending on whether the $\{\phi\}$ are the spatial parts of α or β spin orbitals. The matrix $g^{xc}_\Omega(\mathbf{r}_2;\mathbf{r}'_2)$ can then be expressed in diagonal form using a unitary transformation:

$$g^{xc}_\Omega(\mathbf{r}_2;\mathbf{r}'_2)=2\sum_i^{occ}\varphi_i(\mathbf{r}_2)G^\Omega_{ii}\varphi^*_i(\mathbf{r}'_2) \quad (6)$$

Costales *et al.* emphasized the analogy to the natural orbital decomposition of a density matrix by naming the new basis of single-particle functions φ "domain natural orbitals (DNOs)"[38] and the corresponding eigenvalues as "occupation numbers". As a matter of fact, the choice of atomic basins as domains results in chemically intuitive DNOs like "core orbitals" ($G^\Omega_{ii}=2$), "lone pairs" ($G^\Omega_{ii}\approx 2$) and "broken valences" (or "bond orbitals", $G^\Omega_{ii}<2$) with the corresponding occupation numbers *(e.g. 3)*. Note, however, that again like in density matrices, one can independently diagonalize the α and β spin matrices of Eq. (2). Given that in the present work we only consider closed shell singlet molecules , both matrices are equal and we consider both together.

For the DAFH analysis as applied in this work, the hypervalent bonding region is divided into domains Ω, covering the central iodine atom and the (ipso-) atoms directly bound to it *(Ω_I and Ω_H in 3)*. Based on the form and occupation numbers of the DNOs,

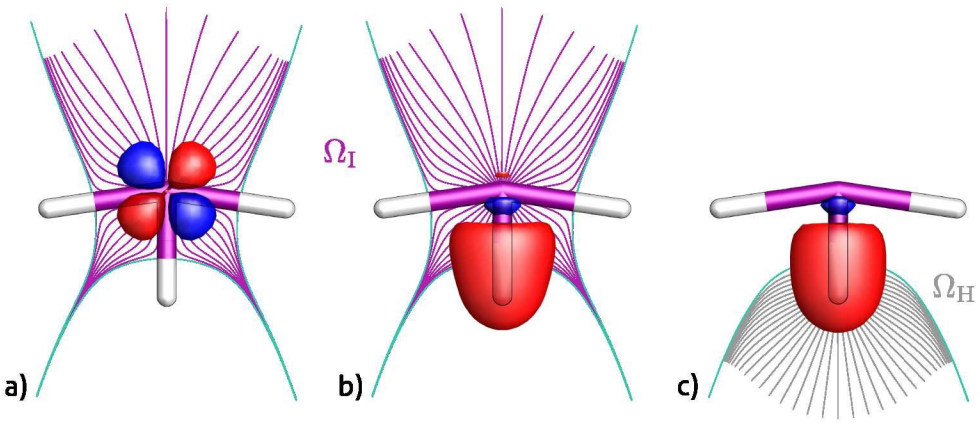

Fig. 3 Illustration of selected domain natural orbitals (DNOs) showing atomic domains Ω of the model compound IH_3: a) a d-orbital of the iodine domain Ω_I, b) a 2-center bonding (2cb) orbital of the iodine domain Ω_I, which reaches into the neighboring hydrogen domain, and c) the corresponding 2cb DNO of the hydrogen domain Ω_H. Whereas the occupation number of the d-orbital is close to 2.0, thus belonging to the iodine core, the 2cb orbitals show "broken valences", i.e. an occupation number typically near 1.0.

core and lone pair orbitals can easily be identified. For the broken valences, visualization gives an indication what bond they participate in *(2cb in 3b & c)*. The sum of the respective occupation numbers will result in a value close to 2.0 for a 2-center bond. In order for a 3-center bond to be established, the broken valences of the central atom domain have to reach into both domains of the *trans*-coordinated ligands to couple with their broken valence counterparts *(see e.g. Figure of abstract)*. Therefore, to determine whether a multicenter bond is present it is sufficient to focus on the iodine domain.

DNO's are moreover not necessarily directed following the bonds a Lewis picture would suggest. In order to obtain such DNO's, an isopycnic transformation[39,40] is performed. This will orient the DNOs to achieve the best possible electron pairing, that, in many cases, corresponds to the Lewis picture. The transformation procedure is based on maximizing the localization sum

$$L = \sum_k \left(G^{\Omega}_{kk}\right)^2 \sum_A \left|S^A_{kk}\right|^2 = \sum_k \left(G^{\Omega}_{kk}\right)^2 L_k \,. \qquad (7)$$

The localization index L consists of the summation over all DNOs of the sum of squared diagonal domain overlap matrix elements over all atoms A. The key behind this transformation is that the matrix $g^{xc}_{\Omega}(\mathbf{r}_2;\mathbf{r}'_2)$ remains unchanged and retains the same type of expression. As the eigenvalues G^{Ω}_{kk} are obviously non-degenerate in most cases, such a transformation is non-unitary and therefore the same expression involving only diagonal elements is only possible when abandoning the orthogonality of the localized DNO's. The localization index $L_k = \sum_A \left|S^A_{kk}\right|^2$ is a measure of deviation from atom-centered orbitals. Thus, the maximization of the localization sum L defines DNO transformations $\widetilde{\varphi}_i = \sum_k X^*_{ik}\varphi_k$, that increase the overlap in bonding regions, and decrease it everywhere else, within the boundaries of paired electrons. Only valence DNOs are (significantly) affected by the transformation, as the core and some lone pair DNOs are already (nearly) fully occupied. If the canonical bond DNOs‡ already show a strong orientation for inter-domain electron coupling, their localized counterparts differ marginally. Hence, the analysis of the evolution of DNOs by isopycnic transformation allows to draw conclusions about the nature of multicenter bonding.

In previous works by Ponec and co-workers on hypervalent compounds[18,19], extensive use was also made of so-called multicenter indices. Considering only two atoms, the bond index is related to exchange-correlation holes like $g^{xc}_{\Omega}(\mathbf{r}_2;\mathbf{r}'_2)$ in a straightforward way. Starting from Eq. (4), a second integration is performed in the following way:

$$k_{\Omega\Omega'} = 2\int g^{xc}_{\Omega}(\mathbf{r}_2;\mathbf{r}'_2) w_{\Omega'}(\mathbf{r}_2)\,\delta\left(\mathbf{r}_2 - \mathbf{r}'_2\right) d\mathbf{r}_2 d\mathbf{r}'_2 \qquad (8)$$

The factor two originates from the fact that we consider both permutations of Ω and Ω' over $\mathbf{r}_1$ and $\mathbf{r}_2$. Note also that here, in the case of a closed shell system we imply that we consider both spins together. The resulting index is known variably as the delocalization index[41], shared electron density index (SEDI)[42], electron sharing index[43] among others, and essentially reflects the degree of bonding between atoms. Especially at the Hartree-Fock (and DFT) level of theory, the values obtained agree remarkably well with classical bond orders. The entire theory of DAFH may be repeated at higher orders, e.g. involving the third order density matrix[44] and in the same fashion as above, bond indices may be computed that span 3, 4, or more domains. These so-called multicenter indices have proven useful to identify important electron delocalization over several atoms like in aromatic systems[45] and hypervalent compounds[18,19]. In the present work, a three-center index is computed involving the iodine atoms and the two atoms bonded in a trans arrangement. The relevant QTAIM based index is given by:

$$k_{\Omega\Omega'\Omega''} = \sum_I \hat{\mathscr{P}}_I \left[\sum_{i,j,k}^{occ,\alpha} \left(S^{I_1}_{ij} S^{I_2}_{jk} S^{I_3}_{ki} \right) + \sum_{i,j,k}^{occ,\beta} \left(S^{I_1}_{ij} S^{I_2}_{jk} S^{I_3}_{ki} \right) \right] \qquad (9)$$

‡ In the present context, the term canonical refers to the standard (orthonormal) DNOs obtained by diagonalization of domain averaged Fermi hole Eq. (4).

The operator $\sum_I \hat{\mathscr{P}}_I$ generates all six possible permutations I without repetition of the three atoms involved in the three-centre bonding. I_1 is then the first atoms in the permutation I and analogously for the other two atoms such that the permutations over three atoms A,B and C are ABC,ACB,BAC,BCA,CAB,CBA. All permutations need to be considered as any bond index should be independent of the atom labelling or sequence. Note that here separate contributions are considered for α and β spin to properly generalise the method to unrestricted treatments. Often, and especially in closed shell systems, evaluation of the multicenter indices may be done more efficiently by considering symmetries. According to Ponec et al.[46], negative values of the 3-center bond index indicate the presence of 3c-4e bonding. Based on an analytical model, the 3-center bond index for an ideal 3c-4e bond should equal -0.1875.[46] However, in that same paper, it is found that for FHF^- the value depends strongly on the quality of the basis set used. Moreover, a Mulliken type index was used and not all permutations are considered. In order to link the present results to those of Ponec et al. Mulliken values were also computed for the reference systems considered by these authors. The relevant indices are:

$$k_{\Omega\Omega'\Omega''} = \sum_I \hat{\mathscr{P}}_I \left[\sum_{\substack{\mu\in I_1 \\ \nu\in I_2 \\ \sigma\in I_3}} \left((P^\alpha S)_{\mu\nu}(P^\alpha S)_{\nu\sigma}(P^\alpha S)_{\sigma\mu}\right) + \sum_{\substack{\mu\in I_1 \\ \nu\in I_2 \\ \sigma\in I_3}} \left((P^\beta S)_{\mu\nu}(P^\beta S)_{\nu\sigma}(P^\beta S)_{\sigma\mu}\right) \right] \quad (10)$$

Here the Greek indices refer to atom centred basis functions on the atoms in the permutation I and $\mathbf{P}^\alpha$, $\mathbf{P}^\beta$ and $\mathbf{S}$ are the charge and bond order matrix for the α and β spin electrons and the overlap matrix in terms of the atom centred basis functions.

We decided to use Kohn-Sham DFT with the B3LYP functional to include a treatment of electron correlation which at least allows to make consitent qualitative conclusions. Correlated wavefunction methods, as used by a number of authors in a similar context,[23,47,48] were not an option because of the size of the systems studied in this work. Also, truncated CI methods depend on the single particle basis and the optimization of the basis is non-trivial[49] or require non-trivial choices of active spaces or may even depend on the use of either relaxed or unrelaxed density matrices[43] such that high accuracy of the result is not automatically guaranteed. One electron approximations could be used[47] but again introduce approximations that may result equally strong as those of using Kohn-Sham orbitals.

3 Computational Details

All *ab initio* computations presented in this work are based on ground state geometries optimized for closed shell singlet states by means of Kohn-Sham density functional theory (KS-DFT), using the quantum chemical package Gaussian 09 (G09 Rev D.01).[50] The B3LYP exchange-correlation functional[51–54] was employed along with the Cartesian aug-cc-pVTZ-PP[55] basis set for the model systems and the Togni reagents, and cc-pVTZ-PP[55] for the diaryliodane series. In order to avoid problems with basis set insufficiencies, which Ponec et al. found responsible for the artificial overestimation of multicenter bonding,[19] we incorporate sufficiently flexible basis sets. Scalar relativistic and scalar spin-orbit effects were considered for the iodine atom by the use of a semi-local effective core potential, the Stuttgart-Koeln-MCDHF-RSC-28-ECP.[56] All energies are given as approximate Gibbs free energies (unless otherwise noted) obtained from vibrational analysis at a temperature of 298.15 K and standard conditions. To confirm the nature of the stationary points, the Hessian was computed for all minima and TS geometries. QTAIM partitioning of the electron density into atomic basins was performed with the AIMALL (Version 14.04.17) program suite.[57] The QTAIM integrations in the presence of pseudopotentials were made possible by proper addition of core densities in the set of natural orbitals leading to the total density. In order to validate the precision of the atomic overlap matrices, we checked that the sum of all matrices leads to the unit matrix with a maximum deviation over all elements of $6.57 \cdot 10^{-4}$ and a root mean square deviation of $3.24 \cdot 10^{-4}$. The program for a posteriori analysis by the DAFH methodology was developed in house, and is available upon request.

4 Results & Discussion

4.1 The Togni Reagents and the Effect of Brønsted-Activation

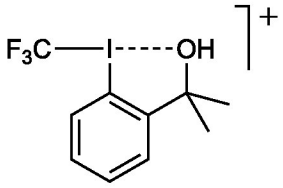

Fig. 4 Activated form of DMTB, protonated at the oxygen atom. The unsymmetrical weakening of the 3-center bond is indicated by the dashed line.

DMTB *(1b)* is considered the "workhorse" among the reagents developed by Togni et al., and is used for the transfer of a trifluoromethyl group to a vast array of nucleophiles.[2] DMTB is a stable aryliodane available off-the-shelf. To access the reactive form of DMTB, an activation process involving Brønsted acids or transition metals is usually performed.[58,59] This activation process has substantial impact on the nature of the 3-center-4-electron (3c-4e) bond, which is oriented along the O–I–C axis *(shaded grey in 1a)*. Already at the structural level, the protonation manifests itself by elongation of the O–I bond, suggesting a weakening of multicenter bonding *(4)*.[4] The change in partial QTAIM charges along the 3-center axis further indicates a substantial modification in the electronic structure *(see 1)*. Even though the protonation occurs at the oxygen atom, surprisingly, its partial charge

	I	O	C
DMTB	0.96	-1.12	1.62
DMTB-$H^{]+}$	0.74	-1.12	1.89

Table 1 QTAIM charges of the iodine center and the ligand ipso-atoms of DMTB before and after protonation.

	canonical					localized				
Ω_I	s	p_z	2cb	3cb	$3cb^{nb}$	s	p_z	2cb	3cb	$3cb^{nb}$
DMTB	1.94	1.87	1.12	0.80	0.14	1.94	1.87	1.10	0.79	0.16
DMTB-H$]^+$	1.96	1.89	1.21	0.97	0.08	1.96	1.89	1.17	1.00	0.08

Table 2 Occupation numbers G_{ii}^{Ω} of the valence DNOs belonging to the iodine domain Ω_I of DMTB before and after protonation, with and without isopycnic localization. Obviously, the effect of the Brønsted-activation is larger than the change introduced by the localization procedure. The lowest population is actually observed in the $3cb^{nb}$ orbital in accordance with the 3c-4e bond model.

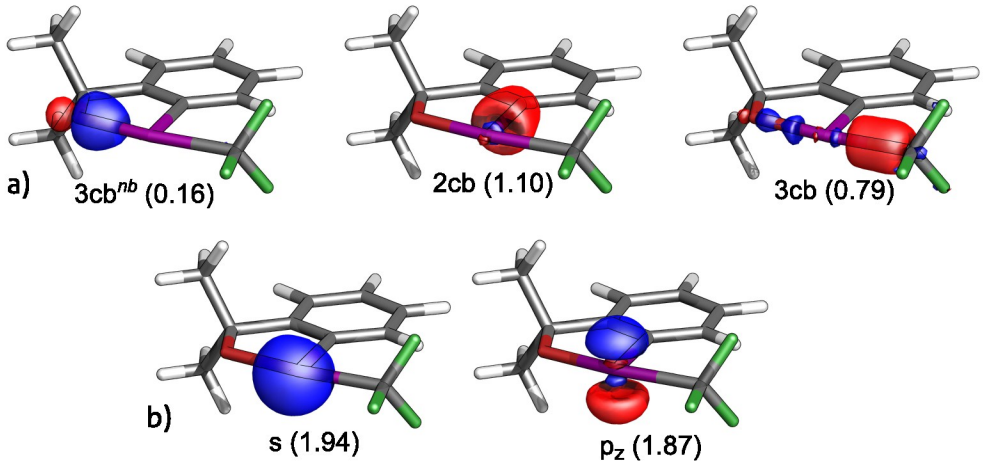

Fig. 5 Localized domain natural orbitals (DNOs) associated with the iodine domain Ω_I of unprotonated DMTB: a) broken valence orbitals: 3-center bonding (3cb), 3-center non-bonding ($3cb^{nb}$) and 2-center bonding (2cb) orbital, b) s- and p_z-lone pair orbitals. The occupation numbers of the DNOs are given in parentheses.

is not affected. This is in contrast to the considerable change in polarization of the I—CF_3 bond. By comparing the magnitude of charges in *1* it is evident that the increase of charge in the carbon atom of CF_3 is compensated by the decrease of charge in the central atom. Obviously, the displacement of the oxygen atom from the 3-center axis influences the opposite bond, which is indirect evidence for delocalized bonding character as proposed in the 3c-4e bond model.

The reactivity of the Togni reagents depends on the characteristics of the hypervalent iodine center, which largely accounts for the unusual chemistry observed. To follow up the introductory arguments about the activation of these reagents, the multicenter character is investigated by focusing on the domain of the central atom. The results of the DAFH analysis of the Togni reagent are listed in *2*, containing the occupation numbers of the valence DNOs of the iodine domain Ω_I. Besides three broken valence orbitals, denoted as 3-center bonding (3cb), 3-center non-bonding ($3cb^{nb}$) and 2-center bonding (2cb) DNOs, there are also two lone pairs corresponding to the orbitals that resemble very much iodine s- and p_z-orbitals *(see 2 & 5)*.

The form of the canonical DNOs of the unprotonated compound resembles the CMOs already presented in *2b*, and, thus, reproduces the 3c-4e bond model. However, visual inspection of the DNOs after isopycnic transformation shows considerably localized bond DNOs *(5)*. While the $3cb^{nb}$ orbital is polarized strongly towards the oxygen atom after the localization procedure, the 3cb DNO still reaches into both ligand domains. The moderate delocalization along with the visible polarization of the 3-center bond orbitals into opposite directions, indicates cleavage of the I—O bond already in the stage of the unactivated reagent. Protonation even amplifies this spatial separation of the 3-center DNOs: *2* shows a rigorous decrease of the $3cb^{nb}$ occupation number, which illustrates the reduced involvement of iodine into the I—O bond. Therefore, the oxygen atom is effectively not participating in the multicenter bond anymore.

In the end, the DAFH analysis anticipates the response to activation of DMTB and leads to an unambiguous picture of independent bond DNOs in the case of DMTB-H$]^+$. Breaking the I—O bond allows entrance and coordination of another substituent, which is crucial for the functionalization reactions performed with Togni reagents.

4.2 Model Systems & Pseudo Jahn-Teller Effect

For a more general understanding of 3-center bonding in λ^3-iodanes in the framework of the DAFH analysis, it useful to examine model systems such as IH_3 and IF_3. Even though electronically these two model compounds represent two extremes, the CMOs show no fundamental difference in their bonding patterns.*) Nevertheless, the role of multicenter bonding appears to be quite different based on the DAFH analysis.

In order for a 3-center bond to be established, the broken va-

*) i.e. we observe an electronic structure as shown in *2a)* for both compounds

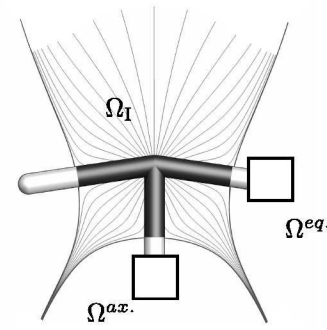

	δ_I	δ_{3cb}	δ_{2cb}	Ω_I 2cb	Ω_I 3cb	Ω_I $3cb^{nb}$	$\Omega^{eq.}$	$\Omega^{ax.}$	
IH_3	+0.80	-0.35	-0.10	1.05	1.06	0.24	1.27	1.02	canon.
				1.04	1.06	0.25	1.27	1.02	local.
IF_3	+1.90	-0.66	-0.58	0.53	0.49	0.09	1.67	1.57	canon.
				0.49	0.31	0.31	1.67	1.57	local.

Table 3 QTAIM charges δ and DAFH occupation numbers G_{ii}^{Ω} of the iodine domain Ω_I and the ligand domains $\Omega^{ax./eq.}$ of the model systems, before and after localization (denoted as canonical and localized, respectively). Note that there is only one entry for the occupation numbers of the symmetry equivalent equatorial domains $\Omega^{eq.}$.

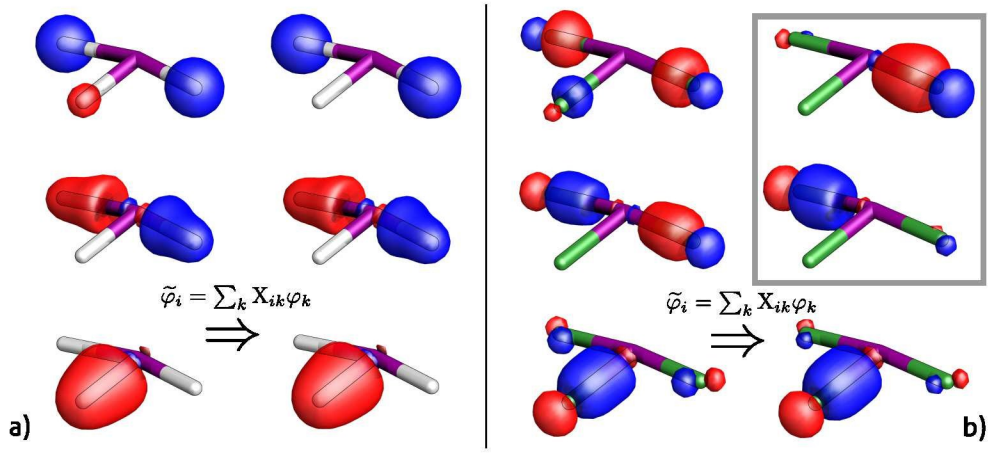

Fig. 6 Bond DNOs of the iodine domain Ω_I belonging to the T-shape configuration of the model systems IH_3 *(a)* and IF_3 *(b)*, before and after localization. The two orbitals in the grey frame of *(b)* take strong 2cb character.

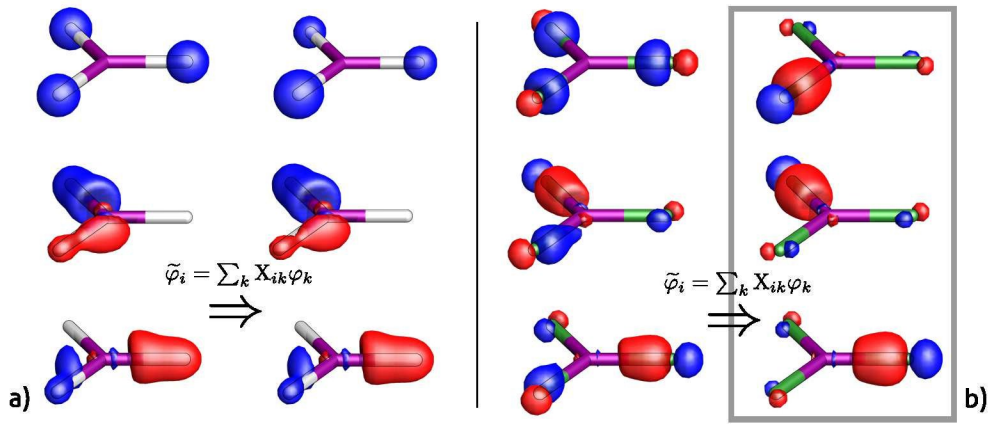

Fig. 7 Bond DNOs of the iodine domain Ω_I belonging to the Y-shape of IH_3 *(a)* and IF_3 *(b)* before and after localization. The three orbitals in the gray frame of *(b)* take strong 2cb character.

lences of the iodine domain Ω_I have to reach into both domains of the *trans*-coordinated ligands *(see e.g. Figure of abstract)*. This is the case for both model compounds before the localization procedure *(left part of 6a & b)*. In comparison to IH_3, the iodine valence DNOs of IF_3 show remarkably low occupation numbers because of its very polar I−F bonds. As a matter of fact, for IF_3 the localization procedure appears to give a fundamentally different picture of the bonding pattern *(3)*. On the other hand, a weak response of the 3-center orbitals upon isopycnic transformation implies that the multicenter nature of the DNOs is intrinsic. Obviously, IH_3 represents a perfect model for the 3c-4e bond, as its orbitals are barely modified *(see 3 and 6)*.

For IF_3 we observe that the isopycnic transformation leads to two equivalent and perfectly localized 2-center bonding orbitals oriented along the 3-center axis. The two bonds are very polar and the corresponding occupation numbers G_{ii}^{Ω} indicate total absence of coupling ($0.31 + 1.67 = 1.98$ electrons per broken valence pair). At the same time, the broken valences of IH_3 only add up to close to four electrons, when considering all of the 3-center DNOs ($1.06 + 1.27 = 2.33$ and $0.25 + 1.27 = 1.52$ for the 3cb and 3cb^{nb} pair, respectively). Thus, by separately summing up the occupation numbers of the 3cb and 3cb^{nb} contributions, we can relate the DAFH analysis directly to the 3c-4e picture. In addition, computation of the 3-center index reveals that for IH_3 ($k_{\Omega_I\Omega^{eq.}\Omega'^{eq.}} = -0.089$) a negative value is found, indicating the presence of a 3c-4e bond. Given the index of IF_3 ($k_{\Omega_I\Omega^{eq.}\Omega'^{eq.}} = -0.045$) this indicator confirms that the 3c-4e bond is weaker.

The index for IH_3 is much smaller than the ideal value postulated by Ponec et al.[46]. The reference values in the latter work should be treated with care, however. First, the ideal value by Ponec et al.[46] is based on a Mulliken formulation and, second, their work does not consider all permutations (even though for three centers this merely scales the values). Hence, our values can differ significantly. The basis set dependence of the Mulliken approach, leads to a 3-center index for FHF^- being already tenfold smaller when computed using a larger basis set compared to a minimal basis set[46]. This basis set dependence is confirmed in our own calculations using Eq. (10), so considering all permutations does not alleviate this problem. QTAIM analysis is far less basis set dependent and we therefor computed QTAIM based 3-center indices (see Eq. (10)) for both the allyl cation and anion, used by Ponec et al.[46] as references for respectively a 3c-2e bond and 3c-4e bond. Our B3LYP/aug-cc-pVTZ calculations confirm that the 3-center index indeed results positive for a 3c-2e bond and negative for a 3c-4e bond. Especially noteworthy is the value for the allyl anion, reference for a 3c-4e bond, where a QTAIM value of -0.112 is found. Compared to this value, IH_3 would indeed exhibit a fairly strong 3c-4e bond. We therefor use the indices of IH_3 and IF_3 as reference for respectively a strongly and a weakly expressed 3c-4e bond in the case of hypervalent λ^3-iodanes.

These observations can be connected to the PJT effect, which is the driving force determining the geometrical arrangement of the ligands.[3] The starting point of the Jahn-Teller distortion is the D_{3h} high symmetry configuration with the ligand atoms arranged in trigonal fashion around the iodine center resulting in a Y-shape structure. By distortion towards a T-shape C_{2v} configuration, a symmetry induced orbital mixing is observed stabilizing the lower symmetry geometry *(see Figure 9 in reference [3])*. The total stabilization amounts to 33.80 kcal/mol in total energy for IH_3, much larger than the 11.17 kcal/mol computed for IF_3. In fact, particularly the 3cb^{nb} orbital profits from increasing covalence, which manifests itself in the reduction of *s*-character upon descending towards the T-shape configuration. For IF_3, the more pronounced hybridization defect of iodine leads to less PJT stabilization. At the same time, the isopycnic transformation results in three equivalent and very polar 2-center orbitals, while in IH_3 the bond DNOs are largely conserved *(see 7)*.

In the end, IF_3 exhibits only a small change in the QTAIM charges of the fluorine atoms upon distortion, as electron-withdrawing ligands enforce localization of the iodine valence orbitals towards their own domain for both configurations. Actually, already the low population of 0.09 electrons of the canonical 3cb^{nb} DNO of IF_3 refers to less pronounced multicenter bonding *(3)*, and the "decoupling" of the 3-center bonds is in stark contrast to the CMO picture.

4.3 Diaryliodane Series

In general, only λ^3-iodanes with at least one aromatic group have sufficient stability to be experimentally isolated.[1] Hence, the most commonly used compounds are diaryliodanes derived from iodonium salts.[22] In this section, we investigate a representative series of 4-methoxyaryl-phenyl-iodanes *(1b)*, some of them already studied under a different focus in previous work.[3,21] The 4-methoxyaryl ligand is often used as directing group, governing the selectivity of the reductive elimination reaction.[60] Here, the goal is to establish a relationship between 3-center bonding and the structural parameters. Therefore, the series of the iodane compounds is such that it covers a broad spectrum of substituents *X (1b)*. The most important results of the DAFH analysis, as well as the barriers of the reductive elimination and the isomerization reactions ($\Delta G^{\circ}_{red.}$ and $\Delta G^{\circ}_{isom.}$), are listed in *4*.

Concerning general trends, we start by visual inspection of the iodine bond DNOs. For illustration, the 3cb and 3cb^{nb} orbitals of two representative compounds are depicted in *8*. The response to a localization procedure of these molecules is quite different. The shape of the bond orbitals of triphenyl iodane *(8a)* keeps significant delocalized 3c-4e bond character, while in bromo-4-methoxyaryl-phenyl-iodane the DNOs localize into separate 2-center bonds. To relate these observations to the 3c-4e picture, we need to separately sum up the occupation numbers G_{ii}^{Ω} of the 3cb and 3cb^{nb} contributions *(see 4)*. If such a "broken valence pair" population deviates considerably from $\sum_{\Omega} G_{ii}^{\Omega} = 2$, the two electron pairs are considered as coupled. This is observed for almost all compounds presented. Only with strongly electron-withdrawing substituents the two pairs are nearly decoupled. Still, given the negative values of $k_{\Omega_I\Omega_X\Omega_{C_3}}$ all diaryliodanes express 3c-4e bonding *(last column in 4)*.

Closer inspection of the isomerization barriers confirms that the most stable compounds of the series are iodanes coordinated by

			Ω_I				Ω_X		Ω_{C_3}		Ω_{C_4}				
X	$\Delta G^\circ_{isom.}$	$\Delta G^\circ_{red.}$	δ_I	2cb	3cb	$3cb^{nb}$	δ_X	$3cb^{nb}$	δ_C	3cb	δ_C	2cb	$\sum G^\Omega_{3cb}$	$\sum G^\Omega_{3cb^{nb}}$	$k_{\Omega_I\Omega_X\Omega_{C_3}}$
Ph	21.16	21.35	0.74	1.08	0.99	0.21	-0.27	1.36	-0.26	1.34	-0.26	0.97	2.33	1.57	-0.071
Ph[a]	21.03	21.09	0.74	1.08	0.99	0.21	-0.26	1.35	-0.26	1.35	-0.26	0.97	2.34	1.56	-0.071
Me	19.39	19.96	0.71	1.07	1.02	0.22	-0.24	1.22	-0.26	1.36	-0.26	1.05	2.38	1.44	-0.074
N_3	10.96	15.26	0.81	1.10	0.94	0.14	-0.37	1.27	-0.29	1.18	-0.28	0.88	2.12	1.41	-0.051
NH_2	14.01	18.58	0.80	1.10	0.92	0.19	-1.11	1.49	-0.27	1.32	-0.28	0.90	2.24	1.68	-0.096
OH	15.63	19.10	0.89	1.08	0.86	0.16	-1.17	1.65	-0.30	1.29	-0.25	0.92	2.15	1.81	-0.072
F	16.90	20.62	0.94	1.08	0.85	0.12	-0.76	1.76	-0.30	1.23	-0.29	0.89	2.08	1.89	-0.051
PMe_2	11.12	11.47	0.57	1.07	1.14	0.22	0.76	1.07	-0.25	1.33	-0.25	0.99	2.47	1.29	-0.074
SPh	10.06	16.49	0.70	1.09	1.00	0.18	-0.35	1.44	-0.27	1.20	-0.27	0.92	2.21	1.61	-0.086
Cl	10.88	19.45	0.78	1.11	0.95	0.14	-0.67	1.69	-0.29	1.17	-0.28	0.87	2.13	1.83	-0.079
Br	9.52	18.85	0.71	1.13	0.99	0.14	-0.64	1.67	-0.28	1.15	-0.28	0.86	2.14	1.81	-0.088

a same as Ph but without methoxy group on the phenyl ring (= triphenyl-iodane)

Table 4 Series of 4-methoxyaryl-phenyl-iodanes: given are the reaction barriers of the isomerization $\Delta G^\circ_{isom.}$ and the reductive elimination $\Delta G^\circ_{red.}$; the AIM charges δ and DAFH occupation numbers G^Ω_{ii} of the different domains after localization. The domains are labeled as follows: iodine Ω_I, substituent Ω_X, 3-center carbon ipso-atom Ω_{C_3}, 2-center carbon ipso-atom Ω_{C_4} *(see atom labels in 1.* In addition, we summed up the associated broken valence pairs $\sum_\Omega G^\Omega_{ii}$.

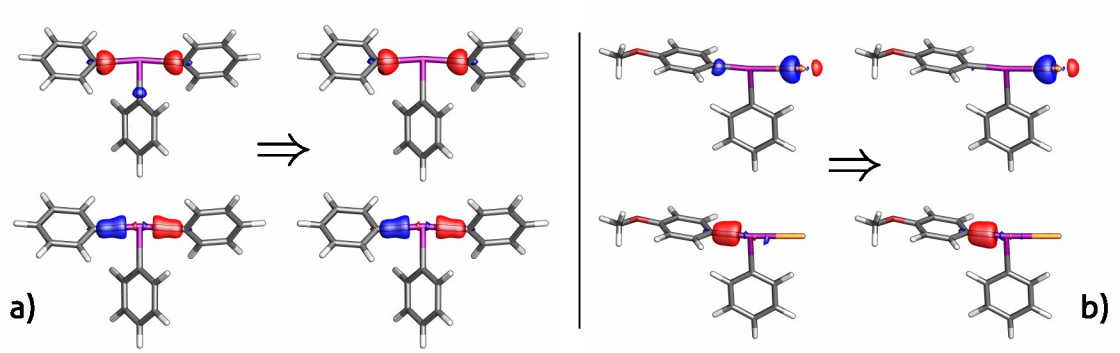

Fig. 8 Evolution of 3cb and $3cb^{nb}$ DNOs of the iodine domain for triphenyl-iodane *(a)* and bromo-4-methoxyaryl-phenyl-iodane *(b)* upon the localization procedure.

three aryl ligands. Focusing on the asymmetric diaryliodanes (e.g. $X = N_3$, NH_2, OH, F), a steady increase of $\Delta G^\circ_{isom.}$ is observed *(see 4)*, however, at a lower level of stabilization. This trend goes along with the electron-withdrawing properties of these ligands. In fact, by breaking the symmetry of the 3-center bond, antibonding character interferes with the $3cb^{nb}$ orbital, which is in turn stabilized by the polarization of the hypervalent bonds *(9)*. The symmetry breaking is also reflected in the contributions of the s and p basis functions in the relevant orbitals *(see 5)*: only in the case of phenyl diaryliodane a total separation of s and p_y contribution occurs, avoiding the mixing of $3cb^{nb}$ and 3cb orbitals.

To complete our discussion, we come back to the subject of activation of the Togni reagent DTMB. In this case, the occupation numbers of the 3cb and $3cb^{nb}$ orbitals are overall smaller than in the diaryliodane series, and the 3-center index amounts to $k_{\Omega_I\Omega_O\Omega_C} = -0.055$ only, an indication of less stable hypervalent bonding. Besides the reported change of polarization, the protonation results in a complete decoupling of the 3-center broken valence pairs and, at the same time, the value of the 3-center index ($k_{\Omega_I\Omega_O\Omega_C} = -0.017$) falls bellow the 3c-4e reference set by IF_3. In the end, the activated DMTB-$H^{]+}$ is ready for the capture of a nucleophile, performing the reductive elimination of the trifluoromethyl group in a subsequent step.[2]

5 Conclusions

The present work shows that λ^3-iodanes do express pronounced 3-center-4-electron bonds, whose strength strongly responds to the kind of ligands bound to the iodine central atom. The sensitivity on the "ligand field" makes these multicenter bonds tunable, which was shown to have direct impact on the reactivity of the compound. The most dramatic example in this regard is the effect of the activation of the Togni reagent by means of protonation: the absolute value of the DAFH 3-center index is reduced from 0.055, indicating the presence of a moderately strong multicenter bond, to 0.017, i.e. only marginal electron coupling across the three atomic centers. The analysis of Domain Averaged Fermi

X	Ph	NH_2	OH	F	PMe_2	SPh	Cl	Br
$\Delta G^{\circ}_{isom.}$	21.16	14.01	15.63	16.90	14.30	10.92	10.88	9.52
p_y in $3cb^{nb}$	0.03	0.32	0.33	0.32	0.07	0.21	0.23	0.20
s in 3cb	0.01	0.22	0.21	0.24	0.06	0.20	0.26	0.27
EN	2.55	3.04	3.44	3.90	2.19	2.58	3.16	2.96

Table 5 Contributions of the p_y and s basis functions to the $3cb^{nb}$ and 3cb iodine DNOs. In addition, the isomerization reaction barrier $\Delta G^{\circ}_{isom.}$ and the Pauling electronegativity (EN)[61] of the ipso-ligand atoms X are shown for comparison.

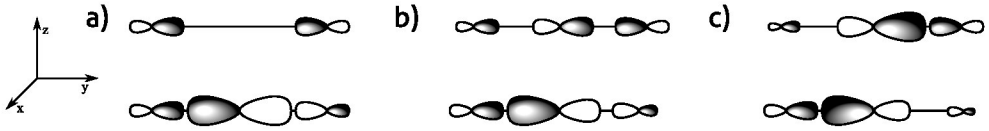

Fig. 9 Impact of breaking the symmetrical ligand sphere in the $3cb^{nb}$ *(top)* and 3cb *(bottom)* DNOs of λ^3-iodanes illustrated by varying the coordination in the 3-center axis: a) two equivalent ligands b) breaking the *trans* symmetry, but still having ligands of similar electronegativity c) two significantly different ligands.

Holes confirms the general 3c-4e multicenter bonding picture of the CMO model, but offers a more detailed picture: electron-rich iodanes exhibit distinct multicenter bonding, whereas electron-withdrawing ligands induce decoupling and localization into electron pairs. These coupling and decoupling patterns allow to relate the multicenter bonding picture with the reactivity of the λ^3-iodanes. The 3-center index offers a quantitative measure to assess the strength of the multicenter bond. Using the allyl anion as a reference (-0.112) for a strongly expressed multicenter bond, IH_3 (-0.089) and IF_3 (-0.045) mark the range in which covers most of the λ^3-iodanes studied in this work.

The most stable and therefore least reactive hypervalent iodine compounds show high isomerization barriers, which, in earlier work, was directly related to the pseudo Jahn-Teller (PJT) effect. We now also show that the distortion to a low symmetry T-shape configuration is accompanied by a significant change in hybridization at the central iodine atom, giving rise to multicenter bonding. The resulting stabilization is most effective in symmetrically *trans*-coordinated and electron-rich λ^3-iodanes, i.e. in those compounds in which the DAFH analysis reveals high population of the 3-center bonding orbital along with a significant 3-center bond index.

On the other hand, it appears that breaking the *trans*-coordination symmetry increases the reactivity of the λ^3-iodanes and opens the range of application for effective functionalization reactions. The impact of inequivalent ligands on multicenter bonding in diaryliodanes shows that the interference of antibonding character with the 3-center bond orbitals will result in unfavorable multicenter bonding. In this situation, the polarization of the hypervalent bonds by electron-withdrawing ligands has a stabilizing influence, and the 3-center bond orbitals are reduced to 2-center bonds.

In conclusion, the application of the DAFH method lead to a better understanding of the structure and bonding in λ^3-iodanes, and will assist the search for novel reagents opening the door for new chemistries.

Acknowledgement

This research was supported by the Swiss National Science Foundation (SNF). Patrick Bultinck acknowledges the Fund for Scientific Research in Flanders (FWO-Vlaanderen) and Ghent University for continuous support. This work has benefited from interesting discussions with A. Togni and O. Sala.

References

1 V. V. Zhdankin and P. J. Stang, *Chem. Rev.*, 2008, **108**, 5299–5358.
2 J. Charpentier, N. Früh and A. Togni, *Chemical Reviews*, 2015, **115**, 650–682.
3 H. Pinto de Magalhães, H. P. Lüthi and A. Togni, *J. Org. Chem.*, 2014, **79**, 8374–8382.
4 O. Sala, H. P. Lüthi and A. Togni, *J. Comp. Chem.*, 2014, **35**, 2122–2131.
5 O. Sala, H. P. Lüthi, A. Togni, M. Iannuzzi and J. Hutter, *Journal of Computational Chemistry*, 2015, 785–794.
6 R. Frei, M. D. Wodrich, D. P. Hari, P.-A. Borin, C. Chauvier and J. Waser, *J. Am. Chem. Soc.*, 2014, **136**, 16563–16573.
7 G. C. Pimentel, *The Journal of Chemical Physics*, 1951, **19**, 446–448.
8 R. J. Hach and R. E. Rundle, *Journal of the American Chemical Society*, 1951, **73**, 4321–4324.
9 R. A. Moss, B. Wilk, K. Krogh-Jespersen, J. T. Blair and J. D. Westbrook, *J. Am. Chem. Soc.*, 1989, **1**, 250–258.
10 M. L. Munzarová and R. Hoffmann, *Journal of the American Chemical Society*, 2002, **124**, 4787–4795.
11 I. B. Bersuker, *Chem. Rev.*, 2001, **101**, 1067–114.
12 M. Atanasov and D. Reinen, *The Journal of Physical Chemistry A*, 2001, **105**, 5450–5467.
13 K.-y. Akiba, *Chemistry of Hypervalent Compounds*, Wiley-VCH, 1999.
14 J. Musher, *Angewandte Chemie International Edition in English*, 1969, **8**, 54–68.
15 W. Kutzelnigg, *Angewandte Chemie International Edition in En-*

glish, 1984, **23**, 272–295.
16 M. Kaupp, in *Chemical Bonding of Main-Group Elements*, Wiley-VCH Verlag GmbH & Co. KGaA, 2014, pp. 1–24.
17 D. E. Woon and T. H. Dunning Jr, *Computational and Theoretical Chemistry*, 2011, **963**, 7–12.
18 R. Ponec and A. J. Duben, *J. Comp. Chem.*, 1999, **20**, 760–771.
19 R. Ponec, G. Yuzhakov and D. L. Cooper, *Theoretical Chemistry Accounts*, 2004, **112**, 419–430.
20 T. H. Dunning Jr, D. E. Woon, J. Leiding and L. Chen, *Accounts of chemical research*, 2012, **46**, 359–368.
21 H. Pinto de Magalhães, H. P. Lüthi and A. Togni, *Org. Lett.*, 2012, **14**, 3830–3833.
22 E. A. Merritt and B. Olofsson, *Angewandte Chemie International Edition*, 2009, **48**, 9052–9070.
23 P. Bultinck, D. L. Cooper and R. Ponec, *J Phys Chem A*, 2010, **114**, 8754–63.
24 M. A. Buijse, *Electron Correlation. Fermi and Coulomb holes, dynamical and nondynamical correlation. Thesis*, Vrije Universiteit, 1991.
25 R. Ponec, *J. Math. Chem.*, 1997, **21**, 323–333.
26 R. Ponec, *Journal of mathematical chemistry*, 1998, **23**, 85–103.
27 R. S. Mulliken, *J. Chem. Phys.*, 1955, **23**, 1833.
28 R. Bader, *Atoms in Molecules: A Quantum Theory*, Pearson Education, 2000.
29 R. F. W. Bader, *Chem. Rev.*, 1991, **91**, 893–928.
30 R. Bader, *Atoms in Molecules. An Introduction*, Oxford University Press, 1990.
31 P. Bultinck, C. Van Alsenoy, P. W. Ayers and R. Carbo-Dorca, *J. Chem. Phys.*, 2007, **126**, 144111.
32 P. Bultinck, P. W. Ayers, S. Fias, K. Tiels and C. Van Alsenoy, *Chem. Phys. Lett.*, 2007, **444**, 205–208.
33 E. Francisco, A. M. Pendas, M. A. Blanco and A. Costales, *Journal of Physical Chemistry A*, 2007, **111**, 12146–12151.
34 P. Bultinck, D. L. Cooper and D. Van Neck, *Physical Chemistry Chemical Physics*, 2009, **11**, 3424–3429.
35 P.-O. Löwdin, *Physical Review*, 1955, **97**, 1474.
36 R. McWeeny and B. Sutcliffe, *Methods of Molecular Quantum Mechanics*, Academic Press, 1969.
37 J. Poater, M. Duran, M. Sola and B. Silvi, *Chem. Rev.*, 2005, **105**, 3911–3947.
38 E. Francisco, A. Martín Pendás and A. Costales, *Phys. Chem. Chem. Phys.*, 2014, **16**, 4586.
39 J. Cioslowski, *Int. J. Quant. Chem.*, 1990, **38**, 015–028.
40 J. Cioslowski, *J. Math. Chem.*, 1991, **8**, 169–178.
41 R. F. W. Bader and M. E. Stephens, *J. Am. Chem. Soc*, 1975, **97**, 7391–7399.
42 R. Ponec and D. L. Cooper, *Journal of Molecular Structure: {THEOCHEM}*, 2005, **727**, 133–138.
43 E. Matito, M. Sola, P. Salvador and M. Duran, *Faraday Discuss.*, 2007, **135**, 325–345.
44 R. Ponec and D. L. Cooper, *International journal of quantum chemistry*, 2004, **97**, 1002–1011.
45 P. Bultinck, R. Ponec and S. Van Damme, *Journal of Physical Organic Chemistry*, 2005, **18**, 706–718.
46 R. Ponec and I. Mayer, *The Journal of Physical Chemistry A*, 1997, **101**, 1738–1741.
47 D. L. Cooper and R. Ponec, *Phys. Chem. Chem. Phys.*, 2008, **10**, 1319–1329.
48 R. Ponec and D. L. Cooper, *Faraday Discuss.*, 2007, **135**, 31–42.
49 D. R. Alcoba, A. Torre, L. Lain, O. B. Oña, P. Capuzzi, M. Van Raemdonck, P. Bultinck and D. Van Neck, *The Journal of Chemical Physics*, 2014, **141**, 244118.
50 M. J. Frisch, G. W. Trucks, H. B. Schlegel, G. E. Scuseria, M. A. Robb, J. R. Cheeseman, G. Scalmani, V. Barone, B. Mennucci, G. A. Petersson, H. Nakatsuji, M. Caricato, X. Li, H. P. Hratchian, A. F. Izmaylov, J. Bloino, G. Zheng, J. L. Sonnenberg, M. Hada, M. Ehara, K. Toyota, R. Fukuda, J. Hasegawa, M. Ishida, T. Nakajima, Y. Honda, O. Kitao, H. Nakai, T. Vreven, J. J. A. Montgomery, J. E. Peralta, F. Ogliaro, M. Bearpark, J. J. Heyd, E. Brothers, K. N. Kudin, V. N. Staroverov, R. Kobayashi, J. Normand, K. Raghavachari, A. Rendell, J. C. Burant, S. S. Iyengar, J. Tomasi, M. Cossi, N. Rega, J. M. Millam, M. Klene, J. E. Knox, J. B. Cross, V. Bakken, C. Adamo, J. Jaramillo, R. Gomperts, R. E. Stratmann, O. Yazyev, A. J. Austin, R. Cammi, C. Pomelli, J. W. Ochterski, R. L. Martin, K. Morokuma, V. G. Zakrzewski, G. A. Voth, P. Salvador, J. J. Dannenberg, S. Dapprich, A. D. Daniels, Ö. Farkas, J. B. Foresman, J. V. Ortiz, J. Cioslowski and D. J. Fox, *Gaussian 09 Revision D.01*, Gaussian Inc. Wallingford CT 2009.
51 A. Becke, *J. Chem. Phys.*, 1993, 5648–5652.
52 C. Lee, W. Yang and R. Parr, *Phys. Rev. B*, 1988, 785–789.
53 S. Vosko, L. Wilk and M. Nusair, *Can. J. Phys.*, 1980, 1200–1211.
54 P. Stephens, F. Devlin, C. Chabalowski and M. Frisch, *J. Phys. Chem.*, 1994, 11623–11627.
55 T. Dunning, *J. Chem. Phys.*, 1989, 1007.
56 K. A. Peterson, B. C. Shepler, D. Figgen and H. Stoll, *J. Phys. Chem. A*, 2006, 13877.
57 T. A. Keith, *AIMALL (Version 14.04.17)*, TK Gristmill Software, Overland Park KS, USA, 2014 (aim.tkgristmill.com).
58 K. Niedermann, N. Früh, R. Senn, B. Czarniecki, R. Verel and A. Togni, *Angew Chem Int Ed Engl*, 2012, **51**, 6511–6515.
59 E. Mejía and A. Togni, *ACS Catal.*, 2012, 521–527.
60 B. Wang, J. W. Graskemper, L. Qin and S. G. DiMagno, *Angew. Chem. Int. Ed.*, 2010, 4079 –4083.
61 J. Dean, *Lange's Handbook of Chemistry*, McGraw-Hill, 15th edn, 1999.